Biophysical Journal
Article

Biophysical Society

Late-Arriving Signals Contribute Less to Cell-Fate Decisions

Michael G. Cortes,[1,2] Jimmy T. Trinh,[3] Lanying Zeng,[3] and Gábor Balázsi[1,4,*]
[1]The Louis and Beatrice Laufer Center for Physical and Quantitative Biology and [2]Department of Applied Mathematics and Statistics, Stony Brook University, Stony Brook, New York; [3]Department of Biochemistry and Biophysics, Center for Phage Technology, Texas A&M University, College Station, Texas; and [4]Department of Biomedical Engineering, Stony Brook University, Stony Brook, New York

ABSTRACT Gene regulatory networks are largely responsible for cellular decision-making. These networks sense diverse external signals and respond by adjusting gene expression, enabling cells to reach environment-dependent decisions crucial for their survival or reproduction. However, information-carrying signals may arrive at variable times. Besides the intrinsic strength of these signals, their arrival time (timing) may also carry information about the environment and can influence cellular decision-making in ways that are poorly understood. For example, it is unclear how the timing of individual phage infections affects the lysis-lysogeny decision of bacteriophage λ despite variable infection times being likely in the wild and even in laboratory conditions. In this work, we combine mathematical modeling with experimentation to address this question. We develop an experimentally testable theory, which reveals that late-infecting phages contribute less to cellular decision-making. This implies that infection delays lower the probability of lysogeny compared to simultaneous infections. Furthermore, we show that infection delays reduce lysogenization by providing insufficient CII for threshold crossing during the critical decision-making period. We find evidence for a cutoff time after which subsequent infections cannot influence the cellular decision. We derive an intuitive formula that approximates the probability of lysogeny for variable infection times by a time-weighted average of probabilities for simultaneous infections. We validate these theoretical predictions experimentally. Similar concepts and simplifying modeling approaches may help elucidate the mechanisms underlying other cellular decisions.

INTRODUCTION

Cells typically live in highly variable environments. They can be exposed to myriads of different ecological and environmental conditions, some of which benefit growth, whereas others cause detriment. To survive, microbes have evolved an arsenal of behaviors to match their environment, such as sporulating in low nutrient conditions (1), utilizing different carbon sources (2,3), and responding to pheromones (4–6), stress (7–9), or other signals (10). Such environmental responses often involve cellular decision-making (11), where cells choose between two or more phenotypes (1,12) to aid population survival in fluctuating environments (13,14). Although higher organisms may rely on a nervous system to match their behavior to specific environments, microbes depend on signal transduction and gene regulatory networks (GRNs) to sense and process external signals to make optimal choices crucial for growth and survival.

External signals carrying environmental information promote cellular decisions by modulating GRN dynamics (15), allowing cells to cope with stress or utilize nutrients efficiently. Over time, the environment may change repeatedly, and a "deliberating" GRN may receive recurrent external signals at variable times. For example, the local concentration of nutrients surrounding an individual cell (16), the arrival of action potentials to neurons (17), or immunogenic signals to dendritic cells (18) may vary temporally. How the timing of external signals influences GRN dynamics and thereby cellular decision-making is not fully understood.

An example of this knowledge gap is in the well-studied bacteriophage λ lysis-lysogeny decision. When bacteriophage λ infects *Escherichia coli* cells, the default outcome is lysis, during which the infecting phages replicate themselves and cause the host cell to burst and release $\sim$100 progeny virions into the environment. These new phages can then go on to infect other susceptible host cells. Alternatively, the infecting phages can opt for lysogeny, a strategy of dormancy in which the phages integrate their viral DNA into the host cell's genome. The infected cell (lysogen) continues to grow and divide normally, duplicating the viral

Submitted March 10, 2017, and accepted for publication September 5, 2017.
*Correspondence: gabor.balazsi@stonybrook.edu
Editor: Mark Alber.
https://doi.org/10.1016/j.bpj.2017.09.012

DNA with each subsequent cell division. Interestingly, the postinfection decision depends strongly on the number of phages infecting a single host cell, a quantity known as the multiplicity of infection (MOI) (19–21). Cells infected at higher MOIs have higher viral gene copy counts, which can bias viral gene expression dynamics toward the lysogenic decision (11,19,20,22–28). Ecological considerations suggest that high MOI signals the scarcity of susceptible host cells, which should increase the chance of lysogeny (26,29). Similar perturbations in gene copy numbers are known to cause significant gene expression changes in other GRNs (25,30).

Once a phage infects a cell, subsequent infections serve as additional signals to the phage λ GRN in the same cell, biasing the postinfection decision toward lysogeny. Yet, lysis-lysogeny models have traditionally considered only simultaneous infections, probably because laboratory experiments try to synchronize infections (21,27,28,31). In the wild, however, phage infection times probably vary significantly due to the multiple steps necessary for phage entry into a host cell (32). Moreover, even the most careful experimental attempts to synchronize infections cannot be perfectly successful. Phages must first bind the LamB complex on the *E. coli* cell surface and then initiate translocation of viral DNA into the host cell's cytoplasm (21,33–35). This process is inherently stochastic as diffusing phages collide with cells randomly and then continue diffusing on the cell surface before irreversibly binding a LamB complex. Even after LamB binding, phage DNA translocates into the host's cytoplasm with random time delays (32,36). Asynchronous translocation times also occur in other phage/host receptor systems (37,38). Although variable infection times should be commonplace in the wild, and even in laboratory experiments, it is unclear how they affect the postinfection decision. Treating the arrival of multiple phages as temporally variable signals incident on a deliberating GRN and studying the subsequent decision outcome should provide general insights into how cellular decision-making depends on the timing of external signals.

In this work, we explore how the timing of infections affects the phage λ lysis-lysogeny decision using mathematical modeling followed by experimental validation. Recent mathematical models of early phage λ development fall into two main categories, depending on the molecular decision-making criterion they assume: 1) first-passage threshold crossing; or 2) sufficient activation of the CII-dependent promoters over some time window (22,27,28,31). Consequently, we apply each of the two decision-making criteria to explore the effects of delayed infections using detailed and simplified models that distinguish the early phase of decision-making from the late phase of decision implementation. All models predict, in a quantitatively consistent manner, that infection delays lower the chance of lysogeny. We validate these predictions experimentally by controlling the infection delays. These findings jointly suggest that CII and Q comprise the core decision-making module of the phage λ gene network that trips the classical CI-Cro genetic switch (39,40) to ensure commitment during the later cell-fate implementation phase. We propose that similar simplifications can be useful in modeling cellular decision-making in other organisms.

MATERIALS AND METHODS

Mathematical and computational models

First, we developed a detailed stochastic model that describes CI, Cro, CII, and Q protein dynamics past the early decision-making phase and also includes viral replication and cell-volume growth (see the Supporting Material). We reduced this detailed model by assuming that all processes are fast except for protein accumulation and degradation (25,31,41). We identified a subsystem of only two proteins (CII and Q) that produced the same chance of lysogeny as the detailed model under specific threshold-crossing criteria (see the Supporting Material). Finally, we obtained a simple ordinary differential equation (ODE) model (see the Supporting Material) that solely concerns the early decision-making dynamics of the GRN in Fig. 1 *A*. This simple model consists of two rate equations in the rescaled variables c and q that we obtained by rescaling CII and Q concentrations by their respective thresholds C_T and Q_T, respectively:

$$\frac{dc}{d\tau} = \mu_c(m/v) - c \tag{1}$$

$$\frac{dq}{d\tau} = \mu_q\left[\frac{m}{v}\left(\frac{1-\Gamma c^4}{1+\Gamma c^4}\right) - \varepsilon + \sqrt{\left(\frac{m}{v}\left(\frac{1-\Gamma c^4}{1+\Gamma c^4}\right) - \varepsilon\right)^2 + \frac{4\left(\frac{m}{v}\right)\varepsilon}{1+\Gamma c^4}}\right] - d_0 q. \tag{2}$$

Here, $d_0 = d_q/d_c$ is the ratio of Q and CII degradation rates; μ_q and μ_c are the rescaled effective *Q* and *cII* transcription rates, respectively, and Γ is the rescaled association constant between CII tetramers and the *paQ* promoter. The parameter ε is a rescaled combination of rate constants from the detailed ODE model. Both CII and Q concentrations depend on two key parameters: m, which denotes the MOI, and $v = V/\overline{V}$, which denotes the initial cell volume, V, rescaled by its cell-population average, $\overline{V} \approx 1.5 \times 10^{-15} L$. We accounted for exponential cell volume increase (growth) by including dilution rates into the degradation rates (see the Supporting Material).

We model the decision as a first-passage process dependent on the concentrations of CII and Q. Guided by the literature (31) and the detailed model (see the Supporting Material), we chose threshold concentrations for CII and Q to be ≈20 nM and 100 nM, respectively. Other parameters (see the Supporting Material) included dissociation constants of $\approx 10^7\ \mathrm{M}^{-1}$, transcription rates of $\approx 1.5\ \mathrm{min}^{-1}$ per gene, translation rates of $\approx 0.5\ \mathrm{min}^{-1}$ per RNA, and combined degradation-dilution rates of RNA and protein of $\approx 0.1\ \mathrm{min}^{-1}$ and $\approx 0.05\ \mathrm{min}^{-1}$, respectively (22,40,42,43). We assumed fast CII degradation due to FtsH (44).

To model delayed infections, we converted m in Eqs. 1 and 2 into a time-dependent variable: $m = m(t)$, increasing it stepwise as each subsequent phage infected the host cell.

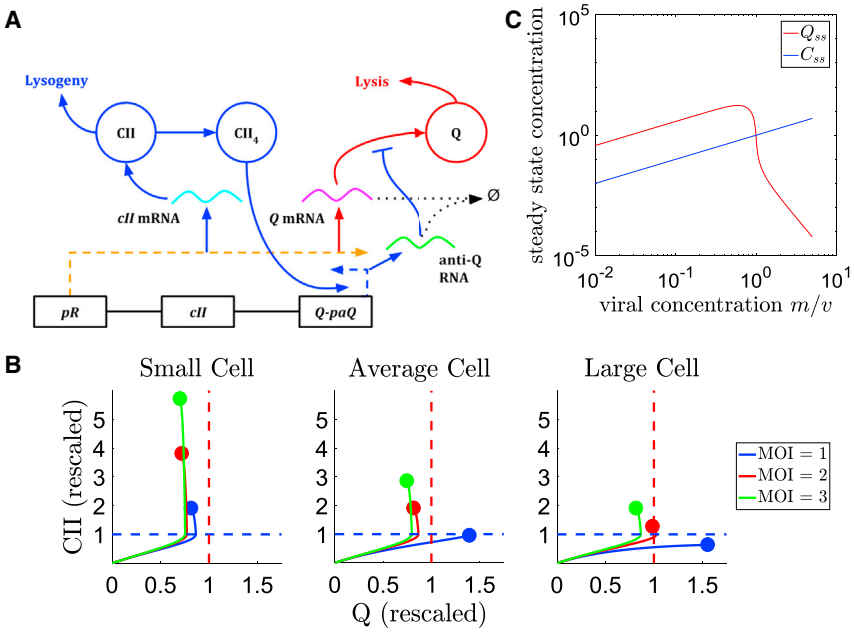

FIGURE 1 Schematic of gene regulatory processes and results of the threshold-crossing model. (*A*) Schematic of the gene regulatory processes in the simple model focused on the early postinfection decision-making dynamics. *cII* and *Q* mRNAs are cotranscribed from the *pR* promoter (*orange dotted line*). *cII* and *Q* mRNAs are translated into CII and Q monomers. CII forms tetramers that activate expression of anti-*Q* mRNA by binding to *paQ*. Activation of *paQ* leads to Q downregulation by binding of *Q* mRNA and anti-*Q* small RNA. Lysogeny occurs if CII reaches its threshold first, which can happen when multiple phages synthesize CII to counteract its fast degradation. Lysis occurs if Q reaches its threshold first. (*B*) CII and Q trajectories through the CII-Q phase space for different MOIs and initial cell volumes. The blue and red dotted lines denote the CII and Q (lysogenic and lytic) thresholds, each normalized to 1 as we rescale c and q by their threshold concentrations C_T and Q_T, respectively. (*C*) Steady-state concentrations of CII and Q versus viral concentration, m/v. Although these steady-state values may not be reached during cellular decision-making, they define attractor states toward which the system gravitates. To see this figure in color, go online.

To obtain stochastic differential equations (SDEs) from the ODES, we added noise terms, ξ, with intensities $D_\xi > 0$ to each deterministic equation. We simulated the SDE system by employing Langevin dynamics with a noise parameter ξ of intensity determined by fitting to experimental data for the probabilities of lysogeny.

For computational simulations of bulk infection experiments we parameterized the exponential distributions of phage arrival times by their mean values, estimated from the average infection time data as ≈3–5 min (see the Supporting Material). To match the experimental data, we calculated the relative fraction of lysogens as the number of lysogens from delayed infection, $N_{\text{delay}}(t)$, versus the number of lysogens from simultaneous infection, $N_{\text{control}}(t)$, according to $[N_{\text{delay}}(t)/N_{\text{delay}}(0)]/[N_{\text{control}}(t)/N_{\text{control}}(0)]$. We sampled infection times from exponential distributions with average arrival times $\langle t_1\rangle \approx 5$ min and $\langle t_2\rangle \approx 3$ min, where subscripts 1 and 2 refer to the first and second batch of infecting phages. Using a phage adsorption assay (see Fig. S11), we estimated that the average infection times should be ∼4 min. Parameter scans gave the best agreement with experimental data for $\langle t_1\rangle = 5$ min and $\langle t_2\rangle = 3$ min, respectively. Other values within the range 3–5 min led to qualitatively similar results.

Deriving the Λ function

In the Supporting Material, we show that the probability of lysogeny is a monotonically increasing function of time-averaged CII levels as $\Lambda = \Lambda(\langle C\rangle_T)$, where $\langle C\rangle_T$ denotes deterministic CII levels averaged over time T for a cell, defined as $\langle C\rangle_T = \frac{1}{T}\int_0^T C(t)dt$. We can break up the integral around the phages' infection times into a sum as $\langle C\rangle_T = \sum_{n=1}^{m}\langle C\rangle_{\Delta t_n}\Delta t_n/T$, where Δt_n equals the time that the cell spends infected by n phages and $\langle C\rangle_{\Delta t_n}$ denotes CII time-averaged over just Δt_n. From here, we can approximate $\Lambda(\langle C\rangle_T)$ linearly as in Eq. 3, since Λ increases monotonically from 0 to 1, and saturates at 1 (see the Supporting Material):

$$\Lambda(\langle C\rangle_T) \approx \begin{cases} \kappa \times \langle C\rangle_T, & 0 \le \langle C\rangle_T \le \langle C\rangle_{\max} \\ 1, & \langle C\rangle_T > \langle C\rangle_{\max} \end{cases}, \qquad (3)$$

where the constant κ is the percentage of lysogeny per concentration of CII, and $\langle C\rangle_{\max}$ is the mean CII level above which the probability of lysogeny is essentially 100%. Indeed, Eq. 3 is supported by simulations using the detailed model (see Fig. S8). Using Eq. 3, we can approximate $\Lambda(\langle C\rangle_T) \approx \kappa\langle C\rangle_T = \sum_{n=1}^{m}\kappa\langle C\rangle_{\Delta t_n}\Delta t_n/T$. In the Supporting Material, we show that $\langle C\rangle_{\Delta t_n}$ is well approximated by $\langle C_n\rangle_T$, which denotes the mean CII averaged over the entire time T for a cell simultaneously coinfected by n phages. Thus, we find that $\kappa\langle C\rangle_{\Delta t_n} \approx \kappa\langle C_n\rangle_T = p_n$, which denotes the probability of lysogeny for n simultaneous coinfections. Consequently, $\Lambda \approx \sum_{n=1}^{m} p_n\Delta t_n/T$.

Time-delayed lysogenization experiment

We diluted phage solution (λ *cI*$_{857}$ *bor::Kan*^{R}) using SM buffer to the average phage input (API) of 8, 6, 4, 3, 2, and 1, calculated as phage concentration/host cell concentration (∼1×10^9 cfu/mL). For each API, the experimental procedures were identical. The following steps give an example of API = 8.

Host *E. coli* MG1655 from an overnight culture was diluted 1:1000 into lysogeny broth (LB) + 0.2% maltose + 10 mM $MgSO_4$ and grown at 37°C with shaking at 265 rpm, until an OD_{600} ∼0.4, where it was then centrifuged (4°C, 2000 × *g*, 10 min) and the pellet was resuspended in one-tenth of the original volume in fresh LB + 10 mM $MgSO_4$ (LBM) to concentrate the cells. There were three groups of infections in each experiment: time delay, mixing control, and unmixed control groups. Twenty microliters of host cells were added to 16 microcentrifuge tubes on ice (seven each for time-delay and mixing-control groups, and two for the unmixed control group). In the first step, for the time-delay group, 10 μL of the "API$_1$" phage solution was mixed with the cells; for the mixing-control group, 10 μL of the API = 8 phage solution was mixed with the cells; and for the unmixed control group, 20 μL of the API = 4 for one tube and 20 μL of the phage solution that is one-half the API of the API$_1$ solution for the second tube were mixed with the cells. The mixtures were placed on ice as all of the samples were being prepared. In the next step, all of the tubes were placed in a 35°C water bath and every 5 min (0–30 min), 10 μL of the "API$_2$" phage solution was added to the time-delay group; 10 μL of SM buffer was added to the mixing control group (time = 0 starts as soon as the cells are initially placed in the water bath); and the unmixed control group was left undisturbed. The temperature and times were chosen

because adsorption occurs faster at higher temperatures and 35°C is still permissive for the function the of cI_{857} temperature-sensitive allele (45). At 30 min, immediately after the final time point, tubes were removed from the water bath and 10 μL of each infection mixture was diluted into 1 mL of prewarmed LB + 0.2% glucose + 10 mM $MgSO_4$ (LBGM) and transferred to a 30°C water shaker at 265 rpm for 30 min. After that, the infection mixtures were diluted appropriately with a single dilution factor, on ice using cold phospshate-buffered saline, and 100 μL of each dilution was spread onto LB + Kan plates and placed in a 30°C incubator overnight for lysogen selection. Colony counts were compared to determine time-delay effects. Host cells were diluted using phospshate-buffered saline and 100 μL of this dilution was plated on LB and grown in a 30°C incubator overnight for the host colony counts. There were three sets of experiments with different mixing ratios for the API_1 and API_2 phage solutions (1:1, 3:1, and 1:3). In the 1:1 experiment, both API_1 and $API_2 = 4$ (second unmixed control tube uses API = 2). In the 3:1 experiment, $API_1 = 6$ and $API_2 = 2$ (second unmixed control tube uses API = 3). In the 1:3 experiment, $API_1 = 2$ and $API_2 = 6$ (second unmixed control tube uses API = 1).

The data for each time point were normalized to the mixing control data of its corresponding time point to account for the effects of diluting the infection mixture at different times. For each experiment, all of these normalized data points were then normalized to the first time point to visualize how the lysogen counts change with delayed phage inputs.

RESULTS

A threshold-crossing model of the phage λ decision-making network

To study the early decision-making phase (as opposed to the late implementation phase), we focused on a relatively simple part of the phage λ GRN. This subnetwork (Fig. 1 *A*) summarizes recent experimental evidence (46) on how threshold-crossing dynamics of the CII and Q viral proteins govern decision-making soon after infection. Specifically, when Q levels cross a particular threshold, late lytic proteins accumulate, driving the assembly of new phages as the cell implements lysis (46). This Q threshold or ultrasensitivity could possibly arise from Q dimerization, Q binding to multiple DNA sites, or Q inhibition by antisense RNA (46–49) expressed from the *paQ* promoter (26). Additionally, earlier studies also indicate that a critical CII threshold exists, possibly arising from CII saturating its cognate host protease FtsH with the assistance of CIII (26,28,50). CII threshold crossing shifts the host cell from its default low-CI (lytic) state to a high-CI (lysogenic) state by activating the *pRE* promoter to drive CI production (28). Ultimately, CI forms dimers and then octamers that repress the *pR* and *pL* promoters to suppress most viral gene expression (including Q and CII) and seal the lysogenic fate (39). Furthermore, threshold CII levels promote Int expression to catalyze viral DNA integration into the host's genome (26,46). If CII levels can trigger these events before Q reaches its own threshold level, then the cell proceeds to lysogenic fate implementation, blocking lytic development.

To examine how threshold crossing drives cell-fate choice during the early cellular decision-making phase, we incorporated the regulatory interactions in Fig. 1 *A* into a simple mathematical model of ODEs that we derived from a detailed model (see Materials and Methods and the Supporting Material). Such simple models are attractive because they are easy to comprehend, require few free parameters, and are amenable to further insightful simplifications (28). Specifically, in this model we tracked the concentrations of 1) CII and Q proteins, 2) *cII*, *Q*, and anti-*Q* mRNA transcripts, 3) free CII tetramers, and 4) CII tetramers bound to the *paQ* promoter. The above experimental findings (46) and the detailed model guided us to assume that the cellular decision is lysis if Q reaches a particular threshold before CII does. Likewise, we assumed that lysogeny occurs if CII reaches its threshold before Q does.

To visualize how MOI and initial cell volume (i.e., at the time of infection) bias the dynamics of CII and Q, we calculated deterministic trajectories through the CII-Q phase space from the ODE model (Fig. 1 *B*). Generally, Q rose to a peak and then decreased, whereas CII increased monotonically. The results indicate that low MOI and high initial cell volumes bias the CII-Q decision-making trajectory toward the lytic region of the phase space that lies above the threshold concentration of Q. Conversely, for high MOI and small initial cell volume the trajectory deviates away from the lytic region of the phase space and heads toward the lysogenic region that lies above the threshold concentration for CII. If the end point of the trajectory lies above both thresholds, the decision depends on which protein crossed its threshold first. These results portray early decision-making as a viral concentration-dependent molecular race between CII and Q toward their thresholds, in agreement with current experimental knowledge of this system (46).

In addition, to study how these early threshold-crossing events trip the classical phage λ CI/Cro genetic switch (39) later, leading to decision implementation, we developed a detailed model that also included the CI and Cro proteins, as well as viral replication and cell growth (see the Supporting Material). This detailed model identified a CII threshold necessary to cross for late, lysogenic CI expression. The lysogenic probability predictions from the two models agreed well with each other (see the Supporting Material).

Molecular mechanisms of phage λ decision-making

Our results so far have suggested that Q and CII both race toward their own thresholds to decide lysis or lysogeny. Somewhat paradoxically, these two proteins are coexpressed, although they control opposing developmental pathways (26). To further understand the molecular mechanisms by which MOI and cell volume affect the bifurcation between lysogeny and lysis despite CII and Q coexpression, we focused on steady-state concentrations of CII and Q. Although the concentrations of CII and Q may not reach their steady-state values, C_{ss} and Q_{ss}, before the decision completes, steady states define attractors toward which the system gravitates during the dynamics. Thus, if C_{ss} is

much larger than Q_{ss}, then the preferred outcome is lysogeny, whereas the reverse is true if Q_{ss} greatly exceeds C_{ss}. Consequently, analyzing the Q_{ss}/C_{ss} ratio for increasing viral concentration (MOI/cell volume or m/v) should reveal how and why it affects the decision.

We found that Q_{ss} initially increased with viral concentration m/v, but then decreased at higher m/v (Fig. 1 *C*). On the other hand, C_{ss} increased proportionally with m/v. At low $(m/v \to 0)$ and high $(m/v \to \infty)$ viral concentrations, the Q_{ss}/C_{ss} ratio had the tendencies

$$\frac{Q_{ss}}{C_{ss}} = \begin{cases} \dfrac{1}{d_0} = \dfrac{d_c}{d_q} \gg 1, & m/v \to 0 \\ 0, & m/v \to \infty \end{cases}. \qquad (4)$$

Indeed, at low viral concentrations $(m/v \to 0)$, Q is much more abundant than CII, since FtsH actively degrades CII, causing CII to be very unstable compared to Q ($d_c \gg d_q$, as the detailed model predicted; see the Supporting Material). Thus, the system will gravitate toward a Q-dominated attractor state, as Q escapes RNA-interference-mediated degradation (Fig. 1 *A*). Conversely, at high viral concentrations $(m/v \to \infty)$, CII dominates in abundance, suppressing Q through RNA interference and ultimately causing lysogeny.

Overall, the model suggests that different degradation rates of CII and Q and the resulting *paQ* activity control the MOI-dependent disparity in CII and Q abundances. Despite their coexpression, CII and Q still promote opposing cell fates, as RNA interference and unequal protein lifetimes control the bifurcation at high and low viral concentrations, respectively.

A stochastic model captures experimentally measured likelihoods of lysogeny

The deterministic model gave insights into how the molecular race and threshold crossing of CII and Q lead to an MOI-dependent decision in single cells without stochasticity. However, phage λ gene expression is inherently stochastic, causing protein-level differences between genetically identical cells in the same environment (11,22,51). Still, traditional experiments typically report only the average chance of lysogeny at each MOI. To enable a comparison with such experimental data while seeking to understand how stochastic gene expression affects cellular decision-making, we transformed the ODE model into an SDE model (see Materials and Methods). We regained the deterministic behavior as the noise intensity decreased toward 0 (see the Supporting Material). To illustrate the effect of stochasticity, we show two realizations of infection outcomes for MOI = 2 in Fig. 2 *B*. These trajectories indicate that although the average trajectory remains lysogenic, random fluctuations cause occasional Q-threshold crossing into the lytic region in phase space. Thus, the outcome of infections can be either lysis or lysogeny due to stochastic gene expression.

Next, to compare these results with experimental data, we calculated the average fraction of lysogenic outcomes from many repeated simulations. We chose biologically reasonable model parameters, adopting them from previously published phage λ GRN models (21) whenever possible. We estimated the remaining parameters by least-squares fitting (see Materials and Methods and Supporting Material; Fig. 2 *A*), comparing the average fraction of lysogenic outcomes from many repeated simulations with experimental data. Despite the model's simplicity, it quantitatively reproduced experimental data on the postinfection decision (Fig. 2 *A*). Stochastic simulations of the detailed model (see the Supporting Material) also reproduced the same data (27,28,31).

Ultimately, the ODE and SDE models concurrently implicate an incoherent feed-forward loop (iFFL) in the postinfection dynamics (Fig. 2 *C*). iFFLs consist of an input gene that activates both a target gene and the target gene's repressor and serve as small computational logic units within natural gene networks (52–54). For high enough repressor levels, iFFLs generate a pulse encoding the fold change of their input signal (54). In phage λ, the input is viral concentration at the time of infection, whereas the repressor and target genes are *cII* and *Q*, respectively. Phage DNA activates both Q and its indirect repressor CII, encoding the viral concentration input into the Q pulse amplitude. This seemingly suggests that Q pulse levels and lysis should increase with viral concentration, in apparent contradiction of experimental observations. However, at low MOI, the host FtsH protease degrades and effectively eliminates the repressor CII (Fig. 2 *C*) from the iFFL, reducing its topology to Q upregulation by only viral concentration to promote lysis. Conversely, high MOI boosts expression and rescues CII elimination from the iFFL soon enough to lower the Q pulse amplitude (54), enabling lysogeny. Thus, the MOI-dependent shift from simple Q upregulation (low CII) to the actual iFFL architecture (high CII) intuitively explains why lysogeny is more likely at high viral concentrations. Once these network architectures cause decision-making, the cell relies on other network modules, such as the CI-Cro bistable switch (27,28,31,39,40) to commit and implement the chosen fate later, as the detailed model indicates (see the Supporting Material) by quantitatively matching the experimental data (21).

Infection delays decrease the chance of lysogeny by lowering CII levels

Armed with a well-calibrated first-passage threshold-crossing model of phage λ decision-making, we proceeded to predict how infection delays alter the chance of lysogeny.

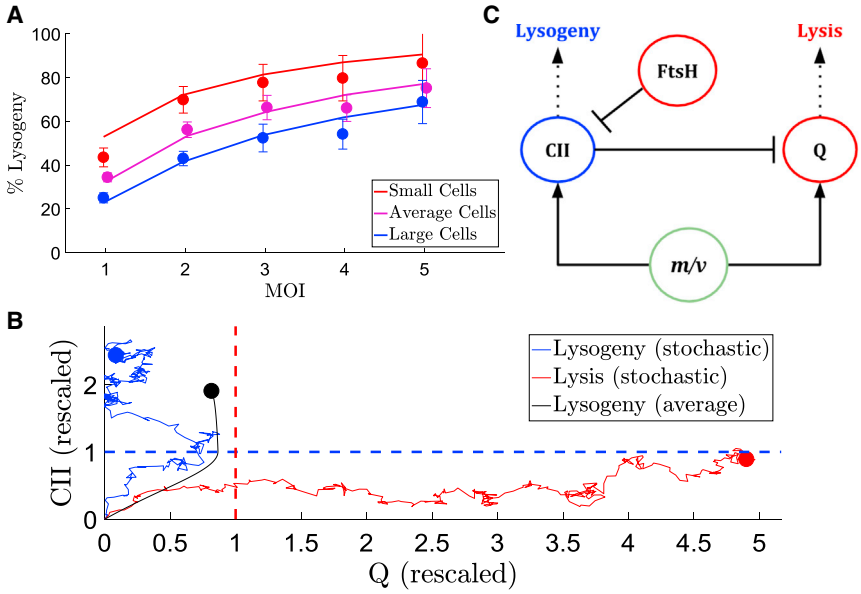

FIGURE 2 Stochastic trajectories and comparison with experimental data. (*A*) Calculated versus experimentally measured probabilities of lysogeny for various MOIs and cell volumes. (*B*) Stochastic trajectories in the CII-Q phase space overlaid on the mean trajectory for MOI = 2 simultaneous infections (*black*) with $v = 1$. On average, the system avoids the lytic region, but stochasticity can randomly push the trajectory into the lytic or the lysogenic region. (*C*) Simplified schematic of an incoherent feedforward loop (iFFL) network motif controlling the lysis-lysogeny decision. As predicted from these results, this simple network motif captures the experimentally measured post-infection decision statistics. This circuitry shows intuitively how viral concentration (m/v) can bias decisions toward lysis or lysogeny. To see this figure in color, go online.

To gain intuitive understanding of this effect, we ran ODE simulations of a double-infection scenario, with the second infection being progressively delayed. As the delay increased, the trajectories headed toward the lytic region in the phase space (Fig. 3 *A*), suggesting that MOI is insufficient to predict the chance of lysogeny. Instead, the decision also depends on the timing of infections: cells infected twice, at two different times, can have substantially different probabilities of lysogeny. Mathematically, the decision will depend on the temporal profile of viral concentration, $m(t)/v$, rather than just m/v.

Next, to determine more generally how variable infection times affect the probability of lysogeny, Λ, we ran stochastic simulations using the SDE model for MOI = m infections with the first $m-1$ being simultaneous while progressively delaying the final, mth infection. Delaying the last infection by time t_m always caused the lysogenic probability $\Lambda(t_m)$ to drop from p_m toward p_{m-1}, where p_m is the chance of lysogeny for m simultaneous infections (Fig. 3 *B*). Essentially, $\Lambda(t_m)$ becomes a weighted average of p_m and p_{m-1}: $\Lambda(t_m) = fp_m + [1-f]p_{m-1}$, with a decreasing weighting function $f = f(t_m)$, where $0 \le f \le 1$. This relationship holds

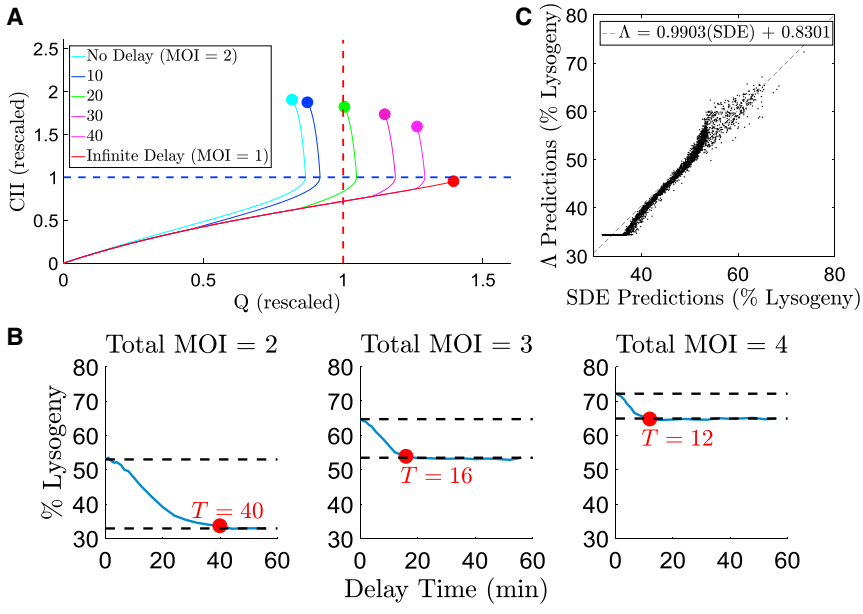

FIGURE 3 Effect of delayed infections on CII-Q dynamics and the probability of lysogeny. (*A*) Deterministic simulations for a total of MOI = 2 infections, but with the second phage's infection time being progressively delayed. Larger delays caused the trajectory to gravitate toward the lytic region. (*B*) Decreasing probabilities of lysogeny versus infection delays for cells infected by a total of $m = 2$, 3, and 4 phages. These results are from stochastic simulations of the simple model (Fig. 1) for a cell simultaneously coinfected first by $m-1$ phages, and with the last (mth) infection being progressively delayed. There is a cutoff time (*red circle*) after which subsequent infections do not affect the cellular decision. (*C*) Approximate agreement (scattering around the first diagonal) between lysogenic probabilities (%) computed for both the time-averaged and first-passage threshold-crossing models (SDE) for 1000 randomly generated sets of infection times for MOIs ranging from 1 to 5. The average deviation between the two models was $\approx 1.2\%$, whereas the maximum deviation was $\approx 8\%$. Parameter scans resulted in an optimal value of $T \approx 24$ min for the cutoff time. These results are also consistent with the detailed model (see the Supporting Material). To see this figure in color, go online.

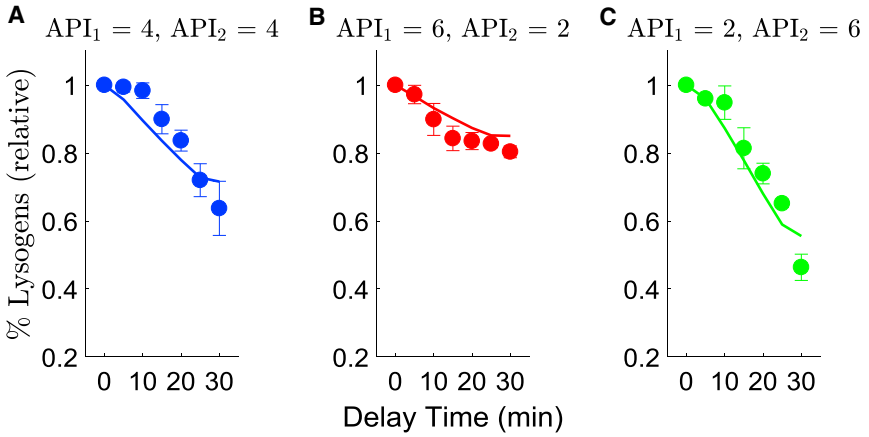

FIGURE 4 Experimental validation of theoretical predictions. Relative probabilities of lysogeny from two consecutive bulk infections with (*A*) equal or (*B* and *C*) different APIs. Infection delays (times of infection with a second batch of phages) generally reduce the percentage of lysogenizing cells relative to the control (simultaneous infection). See the Supporting Material for non-normalized experimental and computational data. To see this figure in color, go online.

even if the first $m-1$ phages do not infect simultaneously (see the Supporting Material). Interestingly, there appears to be a cutoff time after which subsequent infections do not influence the decision. This cutoff precedes cell-fate implementation, which takes 1 h or longer to complete (21). We confirmed these results with the detailed model (see the Supporting Material).

Equivalence of delayed infections to time-weighted average of simultaneous coinfections

Next, we sought to approximate the lysogenic probability $\Lambda(t_m)$ with a simple function using the second type of decision-making criterion, which is threshold crossing of time-averaged (rather than instantaneous) CII levels (22,27). This criterion reflects the fact that CII levels averaged over the decision cutoff time, T (Fig. 3 *B*), should set lysogenic CII-target gene activities. Although the cutoff time in Fig. 3 *B* seems MOI dependent, the real cutoff time could have a complex, stochastic dependence on MOI and infection delays (55) that is difficult to determine. Thus, for simplicity, we assumed an MOI-independent, constant cutoff time, T. Possible physical reasons for this cutoff time are lysogenic prophage integration, or CI-dependent DNA looping (55). After some calculations (see Materials and Methods), we find that the probability of lysogeny is approximately a time-weighted average of lysogenic probabilities for simultaneous infections:

$$\Lambda = \sum_{n=1}^{m} \frac{\Delta t_n}{T} p_n. \tag{5}$$

To test how well the approximation in Eq. 5 matched the results from the first-passage threshold-crossing model, we plotted the predicted probabilities of lysogeny from the two models against each other. The agreement was best for $T = 24$ min (Fig. 3 *C*), which minimizes the sum of squared error between the predictions of the two models. The Λ function approximation also matched results from the detailed model for the same cutoff time (see the Supporting Material). Interestingly, this estimated cutoff time, T, is not far from the experimentally measured time ($\approx$20 min postinfection) of viral DNA integration (55). The remarkable agreement between these models indicates that the approximation of Λ by a time-weighted average of lysogenic probabilities for simultaneous coinfections is justified and reasonable.

Experimental validation of computational predictions

Although both models predict the chance of lysogeny for variable infection times, the corresponding single-cell experimental data are not trivial to collect. Therefore, to predict the chance of lysogeny for some simple, feasible experiments, we developed in silico simulations of two consecutive bulk infections, assuming that 1) phage MOIs follow a Poisson distribution (a frequent, experimentally confirmed assumption in previous studies), and 2) phage infection times follow an exponential distribution (a general assumption for random arrival times in many different contexts) (21,56). We estimated the probability of lysogeny for each cell with the Λ function (Eq. 5) and extracted the other simulation parameters, such as the average arrival rate of the phages and the lysogenic probabilities, p_n, from experimental data (see Materials and Methods and Supporting Material). The model predicted how the chance of lysogeny should decrease with the second bulk infection's delay (Fig. 4).

To validate these predictions experimentally, we performed bulk infections on a population of *E. coli* cells with phages bearing antibiotic resistance markers at an initial API_1 (average MOI per cell), and then, at various later times, we reinfected the same cells at API_2. We then estimated the fraction of lysogens by counting antibiotic-resistant colonies after selective overnight growth, ensuring that

all cells completed their decisions. We normalized these results by the control experiment in which we infected the cells at $API_1 + API_2$ simultaneously only once. The experimental and computational results concordantly show how the fraction of lysogens decreases as we progressively delay the second phage infection (Fig. 4). The simple approximation could capture the experimental data remarkably well, which thus confirm the computational predictions. Overall, these findings suggest steps for coarse-grained approximations that can help with understanding cellular decision-making and other complex cellular processes.

DISCUSSION

In this work, we have examined the phage λ lysis-lysogeny decision's dependence on variable infection times. We show computationally and experimentally that the probability of lysogeny depends inversely on phage infection delays. Infection delays cause this by providing less CII during the decision-making period. We discover a cutoff time after which subsequent infections do not influence the outcome. Mathematically, the probability of lysogeny for delayed infections is a time-weighted average of lysogenic probabilities for simultaneous infections. Thus, the total MOI is insufficient to predict the statistics of cellular-fate choices. Rather, the infection timings also play a key role in the decision, acting as "hidden variables" in addition to cell volume or host-cell physiology (21,57).

Generally, model parameters will depend on environmental conditions. Therefore, future applications of similar models should involve fitting to experimental data while performing parameter scans within biologically relevant limits. Furthermore, the bulk experiments we conducted to examine the impact of delayed infections required scaling up from single cells to cell populations, which involved assumptions about the way phages spread and infect cells in a mixture of cells and phages. In the future, it will be interesting to conduct single-cell measurements to determine how the actual single-cell probabilities of lysogeny depend on variable infection times, which would more directly test these approximations and the existence of a cutoff time.

We demonstrate the power of simple mechanistic models in approximating complex GRN dynamics, showing how such models give meaningful insights into early events driving subsequent complex biological processes. Interestingly, despite the apparent complexity of the phage λ GRN, a switch from simple Q activation to a CII-Q based iFFL (Fig. 2 *C*) intuitively captures experimentally measured decision outcomes. We deduce the simple CII-Q model of early decision-making from a detailed model (see the Supporting Material), which tracks CI, Cro, CII, Q, viral DNA copy numbers, and cell-volume increase until later times, toward cell-fate implementation. The detailed model is quantitatively consistent with experimental lysogenic probabilities (21), as well as with those predicted from the simple CII-Q model, and it indicates the necessity of CII threshold crossing to sufficiently induce CI, repress Q, and thus establish lysogeny. After decision-making, other network modules, such as the CI-Cro genetic switch, subsequently lock in the cell state, ensuring late cell-fate implementation. This perspective of the lysis-lysogeny decision is consistent with earlier studies (46,50) emphasizing the role of transient CII and Q dynamics. Overall, the detailed model in the Supporting Material is consistent with multiple earlier publications and demonstrates how key decision-making molecular events occur in the presence of stochasticity and viral DNA replication, in addition to strengthening the results of the simple model.

Traditional focus has been on the CI-Cro switch being at the core of phage λ decision-making (39). Regarding the CI-Cro switch, we distinguish between two postinfection periods or phases: 1) early decision-making, and 2) late decision implementation. We realize that this distinction may be somewhat arbitrary, but evidence is accumulating (21,26,36,46) that during the early decision-making phase the cell chooses a fate, whereas during the late implementation phase it carries out this chosen fate. From this perspective, CI contributes to the late implementation phase, enforcing lysogeny by shutting down the expression of most phage genes. Likewise, late lytic genes downstream of the pR' promoter ensure lytic implementation after the decision-making events. Although Cro is a crucial regulator of the lytic pathway, it is among the earliest genes expressed right after infection. Therefore, Cro and CI cannot compete during the early decision-making period, because according to the detailed model and the literature (46,58), CI appears only later due to CII threshold crossing. Although the detailed model still allows CI and Cro to compete with each other for *pRM*/*R* promoter access to inhibit or promote late viral gene expression during decision implementation in the fate-committed cell, the outcome of this late competition is already decided before it starts. Once hyperthreshold CII activity causes CI levels to rise sufficiently, CI will displace Cro from this promoter region. Overall, the cell-fate implementation machinery obeys the arbiters of the decision: CII, which directly activates *cI* transcription and phage integration, versus Q, which directly activates transcription of late lytic genes.

Despite their attractive features, simple models can also have shortcomings compared to detailed ones. For example, late Q expression can reverse a lysogenic fate choice (59,60). Although the simple GRN models discussed above cannot capture this phenomenon, it can occur in the detailed GRN model (see the Supporting Material).

CONCLUSIONS

Temporally variable external signals are likely to be quite common and probably contribute to other types of cellular

decision-making, such as neuronal firing, immunogenic activation, or microbial sporulation. It is likely that biological information-processing networks have evolved sensitivity not only to the intensity of external signals, but also to their arrival times, since the timing of signals carries information, and utilizing this information could aid cell growth or survival. More generally, the evolutionary effects of cellular responses to viral infection delays or other signals will be interesting to investigate.

SUPPORTING MATERIAL

Supporting Materials and Methods, twelve figures, and five tables are available at http://www.biophysj.org/biophysj/supplemental/S0006-3495(17)31024-X.

AUTHOR CONTRIBUTIONS

G.B. and M.G.C. designed the study. G.B. and M.G.C. designed network models. M.G.C. performed mathematical and computational modeling. L.Z. and J.T.T. designed the experiments. J.T.T. performed the experiments. All authors wrote the article.

ACKNOWLEDGMENTS

We acknowledge discussions with the members of the G.B. and L.Z. laboratories.

This research was supported by National Institutes of Health National Institute of General Medical Sciences (NIH-NIGMS) grant R01GM107597 and administrative supplement 3R01GM107597-02S1 to L.Z. and G.B., as well as by NIH-NIGMS grant R35GM122561 and by a Laufer Center for Physical and Quantitative Biology endowment to G.B. M.G.C. received additional support from a W. Burghardt Turner Fellowship, and two Turner Summer Research grants at Stony Brook University.

SUPPORTING CITATIONS

References (61–88) appear in the Supporting Material.

REFERENCES

1. Kuchina, A., L. Espinar, …, G. M. Süel. 2011. Temporal competition between differentiation programs determines cell fate choice. *Mol. Syst. Biol.* 7:557.
2. Ozbudak, E. M., M. Thattai, …, A. Van Oudenaarden. 2004. Multistability in the lactose utilization network of *Escherichia coli*. *Nature.* 427:737–740.
3. Ray, J. C. J., M. L. Wickersheim, …, G. Balázsi. 2016. Cellular growth arrest and persistence from enzyme saturation. *PLOS Comput. Biol.* 12:e1004825.
4. Paliwal, S., P. A. Iglesias, …, A. Levchenko. 2007. MAPK-mediated bimodal gene expression and adaptive gradient sensing in yeast. *Nature.* 446:46–51.
5. Jin, M., B. Errede, …, T. C. Elston. 2011. Yeast dynamically modify their environment to achieve better mating efficiency. *Sci. Signal.* 4:ra54.
6. Banderas, A., M. Koltai, …, V. Sourjik. 2016. Sensory input attenuation allows predictive sexual response in yeast. *Nat. Commun.* 7:12590.
7. Dwyer, D. J., P. A. Belenky, …, J. J. Collins. 2014. Antibiotics induce redox-related physiological alterations as part of their lethality. *Proc. Natl. Acad. Sci. USA.* 111:E2100–E2109.
8. Gasch, A. P., P. T. Spellman, …, P. O. Brown. 2000. Genomic expression programs in the response of yeast cells to environmental changes. *Mol. Biol. Cell.* 11:4241–4257.
9. González, C., J. C. Ray, …, G. Balázsi. 2015. Stress-response balance drives the evolution of a network module and its host genome. *Mol. Syst. Biol.* 11:827.
10. Feng, L., S. T. Rutherford, …, B. L. Bassler. 2015. A Qrr noncoding RNA deploys four different regulatory mechanisms to optimize quorum-sensing dynamics. *Cell.* 160:228–240.
11. Balázsi, G., A. van Oudenaarden, and J. J. Collins. 2011. Cellular decision making and biological noise: from microbes to mammals. *Cell.* 144:910–925.
12. Spencer, S. L., S. Gaudet, …, P. K. Sorger. 2009. Non-genetic origins of cell-to-cell variability in TRAIL-induced apoptosis. *Nature.* 459:428–432.
13. Belete, M. K., and G. Balázsi. 2015. Optimality and adaptation of phenotypically switching cells in fluctuating environments. *Phys. Rev. E Stat. Nonlin. Soft Matter Phys.* 92:062716.
14. Balaban, N. Q., J. Merrin, …, S. Leibler. 2004. Bacterial persistence as a phenotypic switch. *Science.* 305:1622–1625.
15. Youk, H., and A. van Oudenaarden. 2009. Growth landscape formed by perception and import of glucose in yeast. *Nature.* 462:875–879.
16. Bennett, M. R., W. L. Pang, …, J. Hasty. 2008. Metabolic gene regulation in a dynamically changing environment. *Nature.* 454:1119–1122.
17. Shu, Y., A. Hasenstaub, …, D. A. McCormick. 2006. Modulation of intracortical synaptic potentials by presynaptic somatic membrane potential. *Nature.* 441:761–765.
18. Macagno, A., G. Napolitani, …, F. Sallusto. 2007. Duration, combination and timing: the signal integration model of dendritic cell activation. *Trends Immunol.* 28:227–233.
19. Kourilsky, P. 1973. Lysogenization by bacteriophage λ. I. Multiple infection and the lysogenic response. *Mol. Gen. Genet.* 122:183–195.
20. Kourilsky, P., and A. Knapp. 1974. Lysogenization by bacteriophage lambda. III. Multiplicity dependent phenomena occuring upon infection by λ. *Biochimie.* 56:1517–1523.
21. Zeng, L., S. O. Skinner, …, I. Golding. 2010. Decision making at a subcellular level determines the outcome of bacteriophage infection. *Cell.* 141:682–691.
22. Arkin, A., J. Ross, and H. H. McAdams. 1998. Stochastic kinetic analysis of developmental pathway bifurcation in phage λ-infected *Escherichia coli* cells. *Genetics.* 149:1633–1648.
23. Herskowitz, I., and D. Hagen. 1980. The lysis-lysogeny decision of phage λ: explicit programming and responsiveness. *Annu. Rev. Genet.* 14:399–445.
24. Kihara, A., Y. Akiyama, and K. Ito. 1997. Host regulation of lysogenic decision in bacteriophage λ: transmembrane modulation of FtsH (HflB), the cII degrading protease, by HflKC (HflA). *Proc. Natl. Acad. Sci. USA.* 94:5544–5549.
25. Mileyko, Y., R. I. Joh, and J. S. Weitz. 2008. Small-scale copy number variation and large-scale changes in gene expression. *Proc. Natl. Acad. Sci. USA.* 105:16659–16664.
26. Oppenheim, A. B., O. Kobiler, …, S. Adhya. 2005. Switches in bacteriophage λ development. *Annu. Rev. Genet.* 39:409–429.
27. Robb, M. L., and V. Shahrezaei. 2014. Stochastic cellular fate decision making by multiple infecting λ phage. *PLoS One.* 9:e103636.
28. Weitz, J. S., Y. Mileyko, …, E. O. Voit. 2008. Collective decision making in bacterial viruses. *Biophys. J.* 95:2673–2680.
29. Gandon, S. 2016. Why be temperate: lessons from bacteriophage l. *Trends Microbiol.* 24:357.
30. Narula, J., A. Kuchina, …, O. A. Igoshin. 2015. Chromosomal arrangement of phosphorelay genes couples sporulation and DNA replication. *Cell.* 162:328–337.
31. Joh, R. I., and J. S. Weitz. 2011. To lyse or not to lyse: transient-mediated stochastic fate determination in cells infected by bacteriophages. *PLOS Comput. Biol.* 7:e1002006.

32. Van Valen, D., D. Wu, …, R. Phillips. 2012. A single-molecule Hershey-Chase experiment. *Curr. Biol.* 22:1339–1343.

33. Löf, D., K. Schillén, …, A. Evilevitch. 2007. Forces controlling the rate of DNA ejection from phage λ. *J. Mol. Biol.* 368:55–65.

34. Moldovan, R., E. Chapman-McQuiston, and X. L. Wu. 2007. On kinetics of phage adsorption. *Biophys. J.* 93:303–315.

35. Rothenberg, E., L. A. Sepúlveda, …, I. Golding. 2011. Single-virus tracking reveals a spatial receptor-dependent search mechanism. *Biophys. J.* 100:2875–2882.

36. Shao, Q., A. Hawkins, and L. Zeng. 2015. Phage DNA dynamics in cells with different fates. *Biophys. J.* 108:2048–2060.

37. García, L. R., and I. J. Molineux. 1995. Rate of translocation of bacteriophage T7 DNA across the membranes of *Escherichia coli*. *J. Bacteriol.* 177:4066–4076.

38. Grayson, P., L. Han, …, R. Phillips. 2007. Real-time observations of single bacteriophage λ DNA ejections in vitro. *Proc. Natl. Acad. Sci. USA.* 104:14652–14657.

39. Ptashne, M. 2011. Principles of a switch. *Nat. Chem. Biol.* 7:484–487.

40. Santillán, M., and M. C. Mackey. 2004. Why the lysogenic state of phage λ is so stable: a mathematical modeling approach. *Biophys. J.* 86:75–84.

41. Alon, U. 2006. An Introduction to Systems Biology: Design Principles of Biological Circuits. CRC press, Boca Raton, FL.

42. Ackers, G. K., A. D. Johnson, and M. A. Shea. 1982. Quantitative model for gene regulation by λ phage repressor. *Proc. Natl. Acad. Sci. USA.* 79:1129–1133.

43. Aurell, E., S. Brown, …, K. Sneppen. 2002. Stability puzzles in phage λ. *Phys. Rev. E Stat. Nonlin. Soft Matter Phys.* 65:051914.

44. Shotland, Y., A. Shifrin, …, A. B. Oppenheim. 2000. Proteolysis of bacteriophage λ CII by *Escherichia coli* FtsH (HflB). *J. Bacteriol.* 182:3111–3116.

45. Zong, C., L. H. So, …, I. Golding. 2010. Lysogen stability is determined by the frequency of activity bursts from the fate-determining gene. *Mol. Syst. Biol.* 6:440.

46. Kobiler, O., A. Rokney, …, A. B. Oppenheim. 2005. Quantitative kinetic analysis of the bacteriophage λ genetic network. *Proc. Natl. Acad. Sci. USA.* 102:4470–4475.

47. Levine, E., and T. Hwa. 2008. Small RNAs establish gene expression thresholds. *Curr. Opin. Microbiol.* 11:574–579.

48. Hoopes, B. C., and W. R. McClure. 1985. A cII-dependent promoter is located within the Q gene of bacteriophage λ. *Proc. Natl. Acad. Sci. USA.* 82:3134–3138.

49. Court, D., L. Green, and H. Echols. 1975. Positive and negative regulation by the cII and cIII gene products of bacteriophage λ. *Virology.* 63:484–491.

50. Little, J. W. 2005. Threshold effects in gene regulation: when some is not enough. *Proc. Natl. Acad. Sci. USA.* 102:5310–5311.

51. Ozbudak, E. M., M. Thattai, …, A. van Oudenaarden. 2002. Regulation of noise in the expression of a single gene. *Nat. Genet.* 31:69–73.

52. Zhang, C., R. Tsoi, …, L. You. 2016. Processing oscillatory signals by incoherent feedforward loops. *PLOS Comput. Biol.* 12:e1005101.

53. Shen-Orr, S. S., R. Milo, …, U. Alon. 2002. Network motifs in the transcriptional regulation network of *Escherichia coli*. *Nat. Genet.* 31:64–68.

54. Goentoro, L., O. Shoval, …, U. Alon. 2009. The incoherent feedforward loop can provide fold-change detection in gene regulation. *Mol. Cell.* 36:894–899.

55. Shao, Q., J. T. Trinh, …, L. Zeng. 2016. Lysis-lysogeny coexistence: prophage integration during lytic development. *MicrobiologyOpen.*.

56. Ellis, E. L., and M. Delbrück. 1939. The growth of bacteriophage. *J. Gen. Physiol.* 22:365–384.

57. St-Pierre, F., and D. Endy. 2008. Determination of cell fate selection during phage λ infection. *Proc. Natl. Acad. Sci. USA.* 105:20705–20710.

58. Reichardt, L., and A. D. Kaiser. 1971. Control of λ repressor synthesis. *Proc. Natl. Acad. Sci. USA.* 68:2185–2189.

59. Semsey, S., C. Campion, …, S. L. Svenningsen. 2015. How long can bacteriophage λ change its mind? *Bacteriophage.* 5:e1012930.

60. Svenningsen, S. L., and S. Semsey. 2014. Commitment to lysogeny is preceded by a prolonged period of sensitivity to the late lytic regulator Q in bacteriophage λ. *J. Bacteriol.* 196:3582–3588.

61. Jain, D., Y. Kim, …, S. A. Darst. 2005. Crystal structure of bacteriophage λ cII and its DNA complex. *Mol. Cell.* 19:259–269.

62. Better, M., and D. Freifelder. 1983. Studies on the replication of Escherichia coli phage λ DNA. I. The kinetics of DNA replication and requirements for the generation of rolling circles. *Virology.* 126:168–182.

63. Dove, W. F., H. Inokuchi, and W. F. Stevens. 1971. Replication control in phage λ. *Cold Spring Harbor Monograph Archive.* 2:747–771.

64. Furth, M. E., C. McLeester, and W. F. Dove. 1978. Specificity determinants for bacteriophage λ DNA replication. I. A chain of interactions that controls the initiation of replication. *J. Mol. Biol.* 126:195–225.

65. Furth, M. E., and S. H. Wickner. 1983. Lambda DNA replication. *Cold Spring Harbor Monograph Archive.* 13:145–173.

66. Taylor, K., and G. Wegrzyn. 1995. Replication of coliphage λ DNA. *FEMS Microbiol. Rev.* 17:109–119.

67. Thomas, R. 1971. Control circuits. *Cold Spring Harbor Monograph Archive.* 2:211–220.

68. Barańska, S., M. Gabig, …, G. Węgrzyn. 2001. Regulation of the switch from early to late bacteriophage λ DNA replication. *Microbiology.* 147:535–547.

69. Mensa-Wilmot, K., K. Carroll, and R. McMacken. 1989. Transcriptional activation of bacteriophage λ DNA replication in vitro: regulatory role of histone-like protein HU of Escherichia coli. *EMBO J.* 8:2393–2402.

70. Wegrzyn, G., A. Wegrzyn, …, K. Taylor. 1995. Involvement of the host initiator function dnaA in the replication of coliphage λ. *Genetics.* 139:1469–1481.

71. Wold, M. S., J. B. Mallory, …, R. McMacken. 1982. Initiation of bacteriophage λ DNA replication in vitro with purified λ replication proteins. *Proc. Natl. Acad. Sci. USA.* 79:6176–6180.

72. Cao, Y., D. T. Gillespie, and L. R. Petzold. 2005. The slow-scale stochastic simulation algorithm. *J. Chem. Phys.* 122:14116.

73. Gillespie, D. T. 1976. A general method for numerically simulating the stochastic time evolution of coupled chemical reactions. *J. Comput. Phys.* 22:403–434.

74. Gillespie, D. T. 2007. Stochastic simulation of chemical kinetics. *Annu. Rev. Phys. Chem.* 58:35–55.

75. Rao, C. V., and A. P. Arkin. 2003. Stochastic chemical kinetics and the quasi-steady-state assumption: application to the Gillespie algorithm. *J. Chem. Phys.* 118:4999–5010.

76. Barik, D., M. R. Paul, …, J. J. Tyson. 2008. Stochastic simulation of enzyme-catalyzed reactions with disparate timescales. *Biophys. J.* 95:3563–3574.

77. Gonze, D., J. Halloy, and A. Goldbeter. 2002. Deterministic versus stochastic models for circadian rhythms. *J. Biol. Phys.* 28:637–653.

78. Sanft, K. R., D. T. Gillespie, and L. R. Petzold. 2011. Legitimacy of the stochastic Michaelis-Menten approximation. *IET Syst. Biol.* 5:58–69.

79. Thomas, P., A. V. Straube, and R. Grima. 2011. Communication: limitations of the stochastic quasi-steady-state approximation in open biochemical reaction networks. *J. Chem. Phys.* 135:181103.

80. Agarwal, A., R. Adams, …, H. Z. Shouval. 2012. On the precision of quasi steady state assumptions in stochastic dynamics. *J. Chem. Phys.* 137:044105.

81. Thomas, P., A. V. Straube, and R. Grima. 2012. The slow-scale linear noise approximation: an accurate, reduced stochastic description of

biochemical networks under timescale separation conditions. *BMC Syst. Biol.* 6:39.

82. Cooper, S. 2006. Distinguishing between linear and exponential cell growth during the division cycle: single-cell studies, cell-culture studies, and the object of cell-cycle research. *Theor. Biol. Med. Model.* 3:10.
83. Folkmanis, A., W. Maltzman, …, H. Echols. 1977. The essential role of the *cro* gene in lytic development by bacteriophage λ. *Virology.* 81:352–362.
84. Svenningsen, S. L., N. Costantino, …, S. Adhya. 2005. On the role of Cro in λ prophage induction. *Proc. Natl. Acad. Sci. USA.* 102:4465–4469.
85. Takeda, Y., A. Folkmanis, and H. Echols. 1977. Cro regulatory protein specified by bacteriophage λ. Structure, DNA-binding, and repression of RNA synthesis. *J. Biol. Chem.* 252:6177–6183.
86. Mensa-Wilmot, K., R. Seaby, …, R. McMacken. 1989. Reconstitution of a nine-protein system that initiates bacteriophage λ DNA replication. *J. Biol. Chem.* 264:2853–2861.
87. Herman, C., T. Ogura, …, P. Bouloc. 1993. Cell growth and λ phage development controlled by the same essential *Escherichia coli* gene, ftsH/hflB. *Proc. Natl. Acad. Sci. USA.* 90:10861–10865.
88. Shotland, Y., S. Koby, …, A. B. Oppenheim. 1997. Proteolysis of the phage λ CII regulatory protein by FtsH (HflB) of *Escherichia coli*. *Mol. Microbiol.* 24:1303–1310.